

The text that follows is a PREPRINT.

Please cite as:

dos Santos Junior, Ulysses Moreira; José Francisco de Carvalho Gonçalves, Reto J. Strasser, Philip Martin Fearnside. 2015. Flooding of tropical forests in central Amazonia: What do the effects on the photosynthetic apparatus of trees tell us about species suitability for reforestation in extreme environments created by hydroelectric dams? *Acta Physiologiae Plantarum* 37, article 166: 1-17.

doi: 10.1007/s11738-015-1915-7

ISSN: 1861-1664

Copyright: Springer Science + Business Media, LLC

The original publication is available at: <http://www.springer.com>

1 **Flooding of tropical forests in central Amazonia: What do the effects on the**
2 **photosynthetic apparatus of trees tell us about species suitability for reforestation in**
3 **extreme environments created by hydroelectric dams?**

4
5 Ulysses Moreira dos Santos Junior^a, José Francisco de Carvalho Gonçalves^{a,*}, Reto J.
6 Strasser^b, Philip Martin Fearnside^c

7
8 ^a Laboratory of Plant Physiology and Biochemistry, National Institute for Research in the
9 Amazon (MCTI-INPA), Manaus, Amazonas, Brazil

10 ^b Bioenergetics and Microbiology Laboratory, University of Geneva, Jussy-Geneva,
11 Switzerland (Reto.Strasser@unige.ch)

12 ^c Coordination for Research in Environmental Dynamics, National Institute for Research in
13 the Amazon (MCTI-INPA), Manaus, Amazonas, Brazil (pmfearn@inpa.gov.br)

14
15 * Corresponding author:

16 National Institute for Research in the Amazon (MCTI-INPA)
17 Av. André Araújo, 2936, Manaus, Amazonas CEP: 69067-375
18 Brazil.

19 E-mail: jfc@inpa.gov.br

20 Tel.: +55 92 3643-1938

21 **Flooding of tropical forests in central Amazonia: What do the effects on the**
22 **photosynthetic apparatus of trees tell us about species suitability for reforestation in**
23 **extreme environments created by hydroelectric dams?**

24

25 Abstract

26 Brazil plans to construct many new hydroelectric dams in the Amazon region. The new
27 conditions of flooding promoted by reservoirs can alter photosynthetic processes, and the
28 study of physiological responses of trees can be used to selected suitable species to reforest
29 these altered areas. The present study analyzed changes in pigment content and photosynthetic
30 performance in flood-tolerant and flood-intolerant species that are common in the floodplains
31 along the Uatumã River and on islands in the reservoir of the Balbina Hydroelectric Dam.
32 Their photosynthetic responses were tested using chloroplast pigment content and chlorophyll
33 *a* fluorescence. Flooding caused a significant reduction in pigment content in all of the three
34 flood-intolerant species and in one of the seven flood-tolerant species studied. Flood-tolerant
35 species were unaffected and neither a change in their chlorophyll contents nor a decrease in
36 the efficiency of energy use in the photosynthetic process was observed. From chlorophyll *a*
37 fluorescence transients (OJIP transients) was calculated the performance index (PI_{ABS}), a
38 parameter derived from the OJIP transient by means of the JIP-test (translation of original
39 fluorescence measurements into biophysical expressions quantifying the stepwise flow of
40 energy through photosystem II). This parameter was a very sensitive indicator of the
41 physiological status of trees under field and was shown to be a particularly sensitive indicator
42 of stress tolerance in flood-intolerant species during inundation, whereas flood-tolerant
43 species had only minor reductions in their photosynthetic performance. We suggest that tree
44 species selection for reforestation around reservoirs can benefit from species-specific
45 measurements of photosynthetic response using the JIP test.

46

47 *Keywords:* chlorophyll *a* fluorescence, hydroelectric dams, JIP-test, performance index, forest
48 tree species, plant stress

49

50

51 1. Introduction

52 Large dams in Brazil's Amazon region currently cover approximately 0.65 million ha.
53 Massive plans for dam building would subject additional forest areas to flood stress: Brazil's
54 2011-2020 electrical expansion plan (Brazil ELETROBRÁS 2011) calls for building 30 dams
55 in the country's Amazon region by 2020, or one dam every four months. This would both
56 cause loss of natural forest area from permanent inundation and die-off of trees in parts of the
57 former upland area that become subject to seasonal flooding.

58 In natural riparian forest the annual flood may last for more than 200 days and attain up
59 to 10 m depth (Junk et al. 1989, 2010). Frequency, duration and intensity of flooding
60 determine which species germinate, establish and reproduce along the flood-level gradient
61 (Junk et al. 1989; Waldhoff et al. 1998; Ferreira et al. 2007, 2009, 2010; Hidding et al. 2014).

62 When a hydroelectric dam is built, new environments appear to which not all tree
63 species are adapted. Reforestation is very important in altered areas and use of native and
64 adapted tree species will inevitably be needed to convert the altered areas into functional
65 riparian forests. To investigate potential species that can be used in restoration projects around
66 hydroelectric reservoirs it is important to know their physiological response under flooding
67 stress.

68 Insights into the photosynthetic metabolism of flood-tolerant species might offer a rapid
69 alternative means of reaching this goal. In general, flooding causes stressful situations that
70 result in typical symptoms such as stomatal closure, reduction of photosynthesis and reduction
71 in pigment content (Gardiner and Krauss 2001; Oliveira and Joly 2010; Mielke and Schaffer
72 2011). Analysis of the pigment composition of leaves is important in plant ecophysiological
73 studies, providing key information about physiological responses to environmental factors
74 such flooding (Kozłowski 2002; Lavinsky et al. 2007; Mielke and Schaffer 2010; Parolin et
75 al. 2010; Duarte et al. 2014). Pigment composition can be a useful indicator due to several
76 characteristics: a) chlorophyll content is altered when a plant undergoes environmental change
77 in its habitat caused either by natural circumstances or anthropogenic disturbance; b)
78 chlorophyll is important in photosynthesis, and c) there is a strong relation between
79 chlorophyll content and the nitrogen concentration in plant leaves.

80 Effects of flooding on the photosynthetic apparatus of individual tropical trees have
81 been studied using such techniques as Chl *a* fluorescence (Waldhoff et al. 2002; Rengifo et al.
82 2005; Parolin et al. 2010; Maurenza et al. 2012; Kissmann et al. 2014). However, many of
83 these studies use only a limited set of parameters such as maximum quantum yield of primary
84 photochemistry (F_v/F_m). New and more specific parameters have been developed using this
85 technique (Strasser et al. 2001, 2004), and these can be used to access tree photosynthetic
86 performance under stressful conditions (Gonçalves et al. 2007; Bussoti et al. 2011; Kalaji et
87 al. 2014). This method is based on high-frequency record of chlorophyll *a* fluorescence
88 emitted by dark-adapted leaves during a short pulse (usually one second) of strong actinic
89 light by fluorometer. Fluorescence kinetics reflect the photochemical efficiency of the
90 photosynthetic apparatus and provide valuable information on functional and structural
91 attributes of components involved in photosynthetic electron transport, mainly photosystem II
92 (Stirbet and Govindjee 2011).

93 The present study aimed to analyze changes in pigment content and photosynthetic
94 performance in flood-tolerant and flood-intolerant species that are common in floodplains
95 along the Uatumã River and on islands in the reservoir of the Balbina Hydroelectric Dam. We
96 hypothesized that flooding will cause: (1) greater reduction in chloroplast pigment content in
97 flood-intolerant species than in flood tolerant species and (2) a change in the fluorescence
98 transients depending on the flood tolerance of each species. If this applies, flood tolerance
99 could be assessed with the postulated methods to provide fast and easy way to obtain

100 information on suitability of species for reforestation in newly created seasonally inundated
101 areas.

102

103 **Materials and methods**

104

105 Study site and species

106

107 The study was conducted in floodplains along the Uatumã River, both upstream and
108 downstream of the Balbina Hydroelectric Dam. The dam is located about 220 km from
109 Manaus in Presidente Figueiredo County, Amazonas state, Brazil (01° 55'S; 59° 28' W).
110 Climate at this site is Amw under the Köppen classification system. In the period of the
111 experiment (2005 – 2007) average annual rainfall was 2392 mm and average values of
112 minimum and maximum temperature were 23.3 and 33.9°C, respectively (Fig 1b and c).
113 Physiological data were collected in two different periods (flooding and non-flooding). The
114 non-flooding period was characterized by reservoir water level varying between 47.64 and
115 48.21 m above mean sea level (January and February of 2006 and 2007) (Fig 1a) and the
116 flooding period was characterized by water level varying between 50.41 and 50.69 m (June
117 and July of 2006 and 2007) (Fig 1a). In the flood period the physiological responses were
118 measured and plants were flooded between 30 and 60 days, flood-tolerant species being
119 exposed to flooding for more time than intolerant species. Flood-tolerant and intolerant
120 species common in natural Uatumã riparian forest and altered areas in the Balbina reservoir
121 were selected and fertile botanical material was collected for identification in the herbarium of
122 the Instituto Nacional de Pesquisas da Amazônia (MCTI-INPA). The intolerant species were
123 all characteristic of early-successional stages, while the tolerant species were from mid- and
124 late-successional stages. Flood-tolerant species were *Nectandra amazonum* Nees (Lauraceae)
125 [Na], *Macrolobium angustifolium* (Benth.) Cowan (Caesalpiniaceae) [Ma], *Alchornea*
126 *discolor* Klotzch (Euphorbiaceae) [Ad], *Brosimum lactescens* (S.Moore) C.C.Berg
127 (Moraceae) [Bl], *Senna reticulata* Willd. (Caesalpiniaceae) [Sr], *Genipa spruceana* Steyerm.
128 (Rubiaceae) [Gs], *Parinary excelsa* Sabine (Chrysobalanaceae) [Pe]. Flood intolerant species
129 were *Cecropia concolor* Willd (Cecropiaceae) [Cc], *Vismia guianensis* (Aubl.) Choisy
130 (Hypericaceae) [Vg] and *Vismia japurensis* Reichardt (Hypericaceae) [Vj]. The classification
131 in tolerant and intolerant species is based on the survival rate under long-term flooding. More
132 details on the studied species are given in Table 1.

133 Ten individuals per species were selected in the study area between July 2005 and
134 January 2006 so that a total of 100 trees were studied. Tree selection followed three criteria:
135 a) all selected individuals were in the adult phase with flowers or fruits present at the time
136 they were marked; b) sampled trees had to be in a seasonally flooded area; c) selected
137 individuals of the same species were located at least 200 m from each other and, if possible,
138 were located on different islands.

139

140 Chloroplast pigment contents

141

142 Chlorophyll *a* (Chl *a*), chlorophyll *b* (Chl *b*) and carotenoid (C_{x+c}) contents of leaves
143 were determined spectrophotometrically by following the methods of Lichetenthaler and
144 Wellburn (1983). For the pigment analyses sun leaves, healthy and completely expanded
145 leaves were collected between 9:00 a.m. to 12:00 p.m. Leaf samples were collected in the
146 middle third of the tree canopy, in sun leaves from all ten individuals of each species. The
147 number of leaves analyzed per individual ranged from 2 (e.g., *Cecropia concolor*) to 10 (e.g.,
148 *Parinary excelsa*). The pigments were extracted in 80% acetone and absorbance of the

149 resulting extracts was measured at 663 nm (Chl *a*), 645 nm (Chl *b*) and 480 nm (C_{x+c}) with a
 150 spectrophotometer (Jenway 6105 UV/VIS). Pigment contents were calculated using the
 151 equations described by Hendry and Price (1993).

152

153 Chlorophyll *a* fluorescence and the JIP-test

154

155 Chlorophyll *a* fluorescence was measured in healthy and completely expanded leaves with a
 156 portable fluorometer (Plant Efficiency Analyser-MK2– 9600, Hansatech, Norfolk, UK). Five
 157 measurements were made for each plant. The data were collected in sun leaves between 9:00
 158 a.m. and 12:00 p.m., using the same instrument. The selected leaves were subjected to a 30-
 159 minute period of adaptation to darkness. Immediately after the dark-adaptation period, the
 160 leaves were exposed to a pulse of saturated light at an intensity of $3000 \mu\text{mol m}^{-2} \text{s}^{-1}$ provided
 161 by an array of six light-emitting diodes (peak 650 nm) for 5 seconds. When the fluorescence
 162 values between F_0 (O) and the maximum F_M (P) are plotted on a logarithmic time scale, a
 163 typical polyphasic rise with two intermediate steps, denoted as “J” and “I” (Strasser and
 164 Govindjee 1992) are clearly revealed, hence the notation “OJIP” for the rapid rise of the Chl *a*
 165 fluorescence transient. A procedure for quantification of OJIP transients is the so-called “JIP-
 166 test,” which represents a translation of stress-induced alterations in the OJIP Chl *a*
 167 fluorescence transients to changes in biophysical expressions quantifying the stepwise flow of
 168 energy through photosystem II (Strasser and Strasser 1995). Fluorescence transients were
 169 recorded from 10 μs to 5 s at 12-bit resolution and the JIP parameters were calculated from
 170 variable fluorescence values at $F_{50\mu\text{s}}$ (considered F_0), $F_{100\mu\text{s}}$, $F_{300\mu\text{s}}$, $F_{2\text{ms}}$, $F_{30\text{ms}}$ and F_M , using
 171 the equations of the JIP-test (Strasser et al. 2004) (see Table 2).

172 The JIP-test was employed to analyze each OJIP transient. The following data from the
 173 original fluorescence measurements were used: maximal fluorescence intensity (F_M); $F_{50\mu\text{s}}$
 174 (considered F_0); fluorescence intensity at 300 μs ($F_{300\mu\text{s}}$) required for calculation of the slope
 175 at the origin of normalized fluorescence rise (M_0) of the relative variable fluorescence (V)
 176 kinetics; the fluorescence intensity at 2ms ($F_{2\text{ms}}$, the J step) denoted as F_J ; and relative
 177 variable fluorescence at 300 μs (V_K), 2 ms (V_J) and 30 ms (V_I). Additional parameters, such
 178 as fraction of oxygen-evolving complex (OEC), relative area between F_M and F_t [= pool size
 179 of electron carriers per reaction center (RC) of photosystem II (PSII) - S_m] and turnover
 180 number of quinone A (Q_A) reductions and re-oxidation (N) are normalized signals calculated
 181 from the measured fluorescence transients (Strasser et al. 2004)

182 The JIP-test represents translation of the original recorded data to biophysical parameters that
 183 quantify the stepwise energy flow through PSII. The parameters which all refer to time zero
 184 (onset of fluorescence induction) are: (i) the specific energy fluxes (per reaction center) for
 185 absorption (ABS/RC), trapping (TR_0 /RC), dissipation at the level of the antenna chlorophylls
 186 (DI_0 /RC) and electron transport (ET_0 /RC). Absorbance (ABS) refers to the absorption of
 187 photons by the chlorophyll molecules in the antenna complex. Part of the absorbed energy
 188 was trapped (TR_0) by the reaction center of PSII (P_{680}) while the remainder was dissipated
 189 (DI_0) in the form of heat and fluorescence. Of the trapped energy a part was converted to
 190 redox energy by electron transport (ET_0) through Q_A and Q_B (Strasser et al. 2000); (ii) the
 191 flux ratios or yields, i.e. the maximum quantum yield of primary photochemistry (ϕ_{P_0}
 192 (TR_0 /ABS)), the efficiency or probability with which a trapped exciton can move an electron
 193 into the electron transport chain further than Q_A (Ψ_0 (ET_0 / TR_0)), the quantum yield of
 194 electron transport (ϕ_{E_0} (ET_0 /ABS)); (iii) the phenomenological energy fluxes (per excited
 195 cross-section of leaf, CS) for absorption (ABS/CS), trapping (TR_0 /CS), dissipation (DI_0 /CS)
 196 and electron transport (ET_0 /CS) derived from the theory of energy flux from biomembranes

197 (Sironval et al. 1981). The fraction of active PSII reaction centers per excited cross-section
198 (RC/CS) is also calculated.

199 The performance index (PI) has been defined as the ratio of two structure-function
200 indexes (SFI). The first, $SFI_{Po(ABS)}$ ($(Chl_{RC}/Chl_{tot}) \times \phi_{Po} \times \Psi_o$), responds to structural and
201 functional PSII events leading to electron transport within photosynthesis (Tsmilli- Michael et
202 al. 1998). The second, $SFI_{No(ABS)}$ ($[1-(Chl_{RC}/Chl_{tot})] (1 - \phi_{Po}) \times (1 - \Psi_o)$), refers to the energy
203 that is dissipated or lost from photosynthetic electron transport, in which Chl_{tot} is the total Chl
204 *a* concentration, and $Chl_{tot} = Chl_{antenna} + Chl_{RC}$. (Strasser et al. 1999). The combination of both
205 structure-function indexes leads to the expression performance index (PI) and when based on
206 absorption of antenna Chls of PSII (PI_{ABS}) can be represented as:

$$207 \quad PI_{ABS} = SFI_{Po(ABS)}/SFI_{No(ABS)} = \{(Chl_{RC}/Chl_{tot})/[1-(Chl_{RC}/Chl_{tot})]\} \times [\phi_{Po}/(1 - \phi_{Po})] \times [\Psi_o$$

208 $/(1 - \Psi_o)]$
209 $= (Chl_{RC}/Chl_{antenna}) \times [\phi_{Po}/(1 - \phi_{Po})] \times [\Psi_o/(1 - \Psi_o)]$, or, in terms of the expression used
210 in the JIP-test

211 (Srivastava et al., 1999): $PI_{ABS} = (RC/ABS) \times [\phi_{Po}/(1 - \phi_{Po})] \times [\Psi_o/(1 - \Psi_o)]$. Thus, PI_{ABS}
212 considers the three main steps that regulate photosynthetic activity by a PSII reaction centre
213 (RC) complex, namely absorption of light energy (ABS), trapping of excitation energy (TR)
214 and conversion of excitation energy to electron transport (ET). The formulas used to calculate
215 the value of each parameter from the original fluorescence measurements and their
216 descriptions are given in Table 2, together with descriptions of all Chl *a* fluorescence
217 parameters analyzed in this study.

218
219 Data analysis

220
221 The experiment was arranged in a completely randomized design in a 10×2 factorial
222 scheme with ten species and two flooding periods (flooding and non-flooding). For each
223 treatment 10 replicates (trees) were used. One-hundred trees were analyzed in each period of
224 flooding. All values were tested for a normal distribution using the Shapiro-Wilk W-Test and
225 homogeneity of variance was determined by using the Brown and Forsythe Test. Differences
226 in chlorophyll content and fluorescence among species were assessed by analysis of variance
227 (ANOVA). Differences in chlorophyll content and fluorescence between the seasons were
228 assessed with a Student's *t*-test for data with parametric distributions, whereas the Mann-
229 Whitney *U*-test was used for non-parametric distributions. All statistical analyses were
230 performed using Statistica for Windows (StatSoft Inc. 2003 East 14th Street, Tulsa, OK,
231 USA).

232
233 **Results**

234
235 Chlorophyll *a* (Chl *a*), chlorophyll *b* (Chl *b*), total chlorophyll (Chl *a+b*) and
236 carotenoids (C_{x+c}) ranged over all species between 617-365, 242-119, 860-585 and 208-138
237 $\mu\text{mol m}^{-2}$ in the non-flooded period and between 628-275, 231-107, 851-382 and 214-121
238 $\mu\text{mol m}^{-2}$ in the flooding period over all species, respectively (Table 3). The effect of flooding
239 on pigment content was significant in *G. spruceana* (*Gs*), *C. concolor* (*Cc*), *V. guianensis* (*Vg*)
240 and *V. japurensis* (*Vj*); pigment contents which decreased by 27, 36, 37 and 31% for Chl *a*;
241 27, 29, 35 and 26% for Chl *a+b*; and 22, 31, 24 and 17% for C_{x+c} (Table 3). Chl *b* only
242 decreased significantly in *Gs* (26%) and *Vg* (29%) (Table 3).

243 All trees exhibited typical polyphasic Chl *a* fluorescence OJIP transients, rising from
244 initial fluorescence (F_o) to maximum fluorescence (F_M) (Fig. 2.A-J). Thus, the original Chl *a*
245 fluorescence transients showed differences in variable fluorescence at 50 μs (F_o), 100 μs

246 ($F_{100\mu s}$), 300 μs ($F_{300\mu s}$), 2ms (F_{2ms}), 30 ms (F_{30ms}) and maximum fluorescence (F_M), with a
 247 marked decrease in F_M in *A. discolor* (*Ad*), *G. spruceana* (*Gs*), *P. excelsa* (*Pe*), *C. concolor*
 248 (*Cc*), *V. guianensis* (*Vg*) and *V. japurensis* (*Vj*) under flooding. The F_O values were constant
 249 in the studied species excepting a decrease in *Gs* and *Pe* and an increase in *Cc* under flooding.
 250 The effects of flooding on JIP parameters were more evident in intolerant species (*Cc*, *Vg*, *Vj*)
 251 and in tolerant species that lose part of their leaves during flooding period (*Ad* and *Gs*) (Fig.
 252 2.A1-J1). In general, the relative areas below the fluorescence curves between F_O and F_M ,
 253 were smaller in plants under flooding and most distinct in *M. angustifolium* (*Ma*) (16%), *Ad*
 254 (16%), *Gs* (45%), *Pe* (30%), *Cc* (41%), *Vg* (37%) and *Vj* (57%). Flooding promoted an
 255 increase in V_K , V_J and V_I levels in *Gs* (34, 17 and 7.7%), *Cc* (72, 38 and 17%), *Vg* (76, 45 and
 256 7%) and *Vj* (56, 40 and 12%) (Figs. 2.F.1, H.1-J.1). Furthermore, lower values of OEC were
 257 observed in *Ad* (4.2%), *Gs* (8.6%), *Cc* (14.0%), *Vg* (17%) and *Vj* (7.8%) under flooding
 258 compared with the non-flooded period.

259 Examination of the specific fluxes (per reaction center; RC) showed increases of 16, 37,
 260 53, 75 and 47% in functional “antenna size” (ABS/RC) and 6, 12, 21, 19 and 10% in trapping
 261 rate of photosystem II (PS II) per RC (TR_O/RC) in *Ad*, *Gs*, *Pe*, *Cc*, *Vg* and *Vj* under flooding,
 262 respectively. In intolerant species increase in “antenna size” was associated with a decrease of
 263 27 (*Cc*), 35 (*Vg*) and 35% (*Vj*) in the electron transport rate per active RC (ET_O/RC). Heat
 264 dissipation per RC (DI_O/RC) was influenced by flooding, especially in *Ad* (38%), *Gs* (108%),
 265 *Pe* (29%), *Cc* (130%), *Vg* (217%) and *Vj* (143%), which had high values of DI_O/RC under
 266 hypoxia. Considering the phenomenological fluxes, a decrease of 18% was observed in the
 267 number of photons absorbed per cross section (ABS/CS) value in *Cc* and increases of 24 and
 268 25% were observed in the ABS/CS values for *Gs* and *Pe*, respectively. In *Gs* and *Pe* the
 269 decrease in ABS/CS was followed by a decrease in trapping rate of PS II per CS (TR_O/CS)
 270 and electron transport rate per CS (ET_O/CS) in inundated trees. Values of heat dissipation per
 271 CS (DI_O/CS) for *Ad*, *Gs*, *Cc*, *Vg* and *Vj* were higher in the flooded period compared to the
 272 non-flooded period.

273 Changes in fluorescence kinetics caused by flooding were more obvious after
 274 normalizing the original OJIP transients between O (F_O) and P (F_M) (Fig. 3.A-J). Normalized
 275 transients for a given flood-tolerant tree under flooded conditions were almost identical to
 276 those under non-flooded conditions. On the other hand, an increase in the J-peak could be
 277 observed in intolerant species such as *Cc*, *Vg* and *Vj* during flooding. The relative
 278 fluorescence between O and P was about 2 ms (J-peak) higher in the intolerant species (Fig 3.
 279 H1-J1) than in the tolerant species under flooded conditions (Fig 3. A1-G1). The differences
 280 in relative fluorescence between O and J showed a K-band formation (Fig. 3. A2-J2). This
 281 was especially present in *Gs*, *Vj*, *Cc* and *Vg* (Fig 3. F2 and J2), but more pronounced in *Cc*
 282 and *Vg* under flooding (Fig. 3. H2 and I2).

283 Associated decreases in maximum quantum yield of primary photochemistry (ϕ_{P_0}) and
 284 increases in maximum quantum yield of non-photochemical de-excitation (ϕ_{D_0}) were
 285 observed in *Gs*, *Cc*, *Vg* and *Vj* (Table 4), indicating a decrease in the efficiency with which
 286 the energy of a trapped exciton is converted into electron transport beyond Q_A^- (Ψ_0) and in the
 287 quantum yield of electron transport beyond Q_A (ϕ_{E_0}) (Table 4). Flooding induced a significant
 288 inactivation of active reaction centers per cross section (RC/CS) in *Ad*, *Gs*, *Pe*, *Cc*, *Vg* and *Vj*
 289 (Table 4).

290 The performance index (PI_{ABS}) [parameter that considers the three main steps that
 291 regulate photosynthetic activity by a PSII reaction center (RC) complex, namely absorption of
 292 light energy (ABS), trapping of
 293 excitation energy (TR) and conversion of excitation energy to electron transport (ET)]
 294 indicated highly significant differences for *Ad*, *Gs*, *Cc*, *Vg*, and *Vj* between the flooded and

295 non-flooded periods (Table 4). The component analyses of “vitality” (PI_{ABS}) revealed that, in
 296 tolerant species that lose part of their leaves during flooding period (*Ad* and *Gs*), the decrease
 297 in PI_{ABS} was influenced more by the $[\phi_{P_o}/(1 - \phi_{P_o})]$ term than by the $[\Psi_o/(1 - \Psi_o)]$ term or by
 298 density of RCs per chlorophyll (RC/ABS). On the other hand, decrease in PI_{ABS} in the flood-
 299 intolerant species (*Cc*, *Vg*, *Vj*) was more strongly influenced by the $[\Psi_o/(1 - \Psi_o)]$ term than by
 300 the $[\phi_{P_o}/(1 - \phi_{P_o})]$ and RC/ABS terms (Fig. 4). The log function of the relative performance
 301 index [$\log(PI_{ABS})_{rel} = \log(PI_{ABS(flooded)}/PI_{ABS(not-flooded)})$] was linearly correlated ($R^2 = 0.982$)
 302 with the log function of the relative electron transport activity [$\log(ET_o/ABS)_{rel} =$
 303 $\log(ET_o/ABS_{(flooded)}/ET_o/ABS_{(not-flooded)})$] (Fig. 5). Flood-intolerant species (*Cc*, *Vg* and *Vj*)
 304 had low negative values, whereas flood-tolerant deciduous species (*Ad* and *Gs*) had
 305 intermediate negative values and flood-tolerant evergreen species (*Na*, *Ma*, *Bl*, *Sr* and *Pe*) had
 306 the highest values of $\log(PI_{ABS})_{rel}$ and $\log(ET_o/ABS)_{rel}$ (Fig. 5).

307 Discussion

308 Reduction in pigment content is a typical stress symptom due to oxidative processes in
 309 the chloroplast, resulting in either slow synthesis or rapid breakdown of pigments (Smirnoff
 310 1993). The results demonstrate that flooding promotes reduction in chloroplast pigment
 311 content in flood-intolerant species but did not impact the pigment contents of tolerant tree
 312 species that are naturally exposed to flooding. These results corroborate the first hypothesis of
 313 this study: that chloroplast pigment reduction will be greater in flood-intolerant species.
 314 According Parolin (2001a) and Waldhoff et al. (1998), some species can show reduction in
 315 pigment content, and the reductions in some species are related to leaf age. However, some
 316 species (e.g., *Senna reticulata*) can have higher pigment content under flooding; this may be
 317 related to strong production of adventitious roots and result from enhanced water supply
 318 (Parolin 2001a). The Chl *a* was more susceptible to degradation by flooding than Chl *b*,
 319 leading to a significant decrease in the Chl *a*/Chl *b* ratio, especially in the two flood-intolerant
 320 species (*Cc* and *Vj*). Severe pigment degradation could also be assessed visually, since the
 321 three species (*Cc*, *Vg* and *Vj*) had stress symptoms such as epinasty and early senescence
 322 (observed for these species in the field), which are usually induced by an increase in ethylene
 323 concentration during flooding (Yamamoto and Kozlowski 1987). None of the flood-tolerant
 324 species in this study, with the exception of *Gs*, showed any significant reduction in
 325 Chlorophyll *a+b* content during inundation, indicating a good adaptation of the
 326 photosynthetic apparatus to flooding. However, the significant decrease in pigment content in
 327 the flood-tolerant species *Gs* could be due to the fact that the flooded period coincides with
 328 the time when this species sheds leaves and immediately re-flushes new leaves. Similar
 329 behavior has been found for the flood-tolerant evergreen species *Symmeria paniculata* in the
 330 Central Amazon, in which changes in chlorophyll content were associated with leaf age,
 331 rather than with high water level (Waldhoff et al. 2002).

332 In the present study evidence was found of changes in performance of the electron pool
 333 size of PSII during flooded conditions, including parameters such as Q_A , Q_B and PQ . This is
 334 typically indicated by the relative areas below the fluorescence curves between F_o and F_m
 335 (Joliot and Joliot 2002). The shape of the OJIP transients indicated sensitivity to stress in
 336 intolerant species during inundation, whereas under non-flooded conditions the Chl *a*
 337 fluorescence intensity curves of healthy leaves did not exhibit typical polyphasic OJIP
 338 transients. Furthermore, normalizing the Chl *a* fluorescence transient at each step between F_o
 339 and F_M revealed a rapid rise in the Chl *a* fluorescence transient between O and P in the flood
 340 intolerant species *Cc*, *Vg* and *Vj* during inundation, but this was not present in the species
 341 adapted to seasonal flooding. This rapid rise of about 2 ms (J-peak) in the fluorescence
 342

344 intensity of intolerant species is most probably induced by blocking electron transport
 345 between Q_A and Q_B (Tóth et al. 2005), by inhibition of primary charge separation, and by an
 346 accumulation of the fraction of primary quinone electron acceptors in PSII in the reduced
 347 state Q_A^- (Haldimann and Strasser 1999). The difference in fluorescence transients
 348 corroborates our second hypothesis, namely that change in these transients depends on the
 349 flood tolerance of the species.

350 It is generally assumed that stomatal closure, which can occur during flooding, causes
 351 decreased photosynthesis and consequently a decrease in the dissipation of latent heat by
 352 transpiration (Kozłowski 1997; Mielke and Shaffer 2010). Over a long period of flooding it is
 353 possible that alterations in carboxylation enzymes and pigment degradation could also
 354 decrease carboxylation efficiency and apparent photosynthetic quantum yield of flooded
 355 plants (Pezeshki 1994).

356 The K-band is a good indicator of stomatal closure and hence reduced assimilation rates
 357 for plants growing naturally in ecosystems in hot, dry environments (Srivastava 1997). In our
 358 study, hypoxia promoted the formation of a K-band between 0.24 and 0.36 ms in intolerant
 359 species (*Cc*, *Vg* and *Vj*) in the flooding period. According to Strasser (1997), a pronounced K-
 360 band can be explained by an imbalance within PSII when the rate of electron flow from P680
 361 to the acceptor side of PSII exceeds the rate of electron flow from the donor side of PSII to
 362 P680. This is usually associated with a dissociation of the OEC and an impairment of the
 363 electron chain (Lazár 2006) and leads to a significant reduction in assimilation rates. The
 364 intolerant species (*Cc*, *Vg* and *Vj*) presented a high reduction in photosynthetic rate during
 365 flooding compared to the tolerant species (See Santos Junior et al. 2013).

366 Values reported for photosynthetic yield (ϕ_{P_0}) in other studies on tropical species in
 367 waterlogged sites vary from no changes in ϕ_{P_0} during flooding (Parolin, 2001b) to significant
 368 changes in ϕ_{P_0} (Rengifo et al. 2005). The values of ϕ_{P_0} we found were between 0.58 and 0.76
 369 for intolerant species (*Cc*, *Vg* and *Vj*) under non-flooded conditions, while these species had
 370 average values of 0.61, 0.58 and 0.59, respectively, when exposed to inundation for about 30
 371 days. Similar values between 0.73 and 0.78 were reported for *Acosmium nitens*, *Campsiandra*
 372 *laurifolia* and *Symmeria paniculata* during the dry season, which also decreased under the
 373 influence of high water levels (Rengifo et al. 2005). Waldhoff et al. (2002) measured a
 374 maximum ϕ_{P_0} of 0.66 in leaves of *Symmeria paniculata*, with values reaching levels between
 375 0.1 and 0.4 in leaves submerged at greater depth (1-7.8 m) after 160-180 days of
 376 submergence.

377 Lower values of ϕ_{P_0} in *Ad*, *Gs*, *Vg* and *Vj* under flooded conditions were induced by the
 378 decrease in F_M values, whereas in *Cc* they were induced by the increase in the F_0 value. In
 379 addition, lower values of ϕ_{P_0} in *Ad*, *Gs*, *Cc*, *Vg* and *Vj* under flooding compared to the non-
 380 flooded period can be explained, in part, by inactivity of the reaction center and increase silent
 381 centers (or heat-sink centers), which would have favored greater dissipation of energy as
 382 demonstrated by high values of ϕ_{D_0} . According to Hermans et al. (2003), silent centers absorb
 383 light in the same way as active RCs but are not able to store the excitation energy as redox
 384 energy, dissipating their total energy in the form of heat. Thus, decrease in fraction of active
 385 RCs can be considered as a down-regulation mechanism to dissipate the excess of absorbed
 386 light in a controlled way (Bussotti et al. 2007; Strasser et al. 2004). Down regulation in *Ad*, *Gs*
 387 and *Pe* may apply, but the decrease in RC/CS in *Cc*, *Vg* and *Vj* could also result from
 388 degradation caused by earlier senescence observed in these species under flooding. This was
 389 indicated by high values of dissipation rate per reaction center (DI_0/RC).

390 Low values of ϕ_{P_0} , *Gs*, *Cc*, *Vg* and *Vj* were associated with lower values of Ψ_0 in the
 391 flooded period, as compared to the non-flooded period, indicating a reduction in the
 392 plastoquinone pool in an oxidized state and reoxidation inhibition in Q_A^- . This indicates,

393 besides the loss of energy to Q_A , a significant loss of excitation energy beyond Q_A (Force et
 394 al. 2003). The results demonstrate that intolerant species inundation had a stronger effect on
 395 efficiency of electron transport of excitation energy beyond Q_A (Ψ_o) than did the maximum
 396 quantum yield of primary photochemistry (ϕ_{P_0}). In addition, as a consequence of ϕ_{P_0} and Ψ_o
 397 having low values, G_s , C_c , V_g and V_j all had significantly lower probability of an absorbed
 398 photon moving an electron beyond Q_A (ϕ_{E_0}) in the flooded period, as compared to the non-
 399 flooded period. Loss of efficiency in photosynthetic electron transport (as discussed for
 400 pigment content) could have resulted from ethylene production induced by flooding causing
 401 epinasty and from earlier senescence. Thus, especially in intolerant species, earlier senescence
 402 could have been accompanied by dismantling of thylakoid membranes, characterized by
 403 chlorophyll degradation, loss of photosynthetic electron-transport activity, and breakdown of
 404 the stromal proteins in the chloroplasts (Noodén et al. 1997). Damage provoked in parts of
 405 PSII, such as the light-harvesting complex II (LHC II), water splitting or oxygen evolving
 406 complex (OEC) and the reaction center (RC), or blockage in any other part of the electron
 407 transport to photosystem I (PS I), will affect carbon assimilation.

408 The performance index on an absorption basis (PI_{ABS}) combines into a single multi-
 409 parametric expression the three independent functional steps (density of RCs in the
 410 chlorophyll bed, excitation energy trapping and conversion of excitation energy to electron
 411 transport) that regulate photosynthetic activity by a PSII reaction center complex (Strasser et
 412 al. 2004; Tsimilli-Michael et al. 2000). PI_{ABS} was shown to be a sensitive parameter for
 413 probing the effects of flooding in tolerant and intolerant species. We observed that intolerant
 414 species showed a more intense decrease in PI_{ABS} than did tolerant species during inundation.
 415 Low values of PI_{ABS} were more affected by decrease in efficiency of conversion of excitation
 416 energy to electron transport [$\Psi_o/(1 - \Psi_o)$] than by decrease in efficiency of primary
 417 photochemistry [$\phi_{P_0}/(1 - \phi_{P_0})$] or by decrease in reaction centers per chlorophyll (RC/ABS).
 418 This result suggests that the large decrease in [$\Psi_o/(1 - \Psi_o)$] is due to the large increase in
 419 fluorescence at the J-step of the OJIP fluorescence transient (Strauss et al. 2006).

420 Comparing the sensitivity of PI_{ABS} and F_v/F_M to flooding, we found that mean values of
 421 PI_{ABS} were more sensitive and robust than mean values of F_v/F_M . These results corroborated
 422 our third hypothesis: that the new fluorescence parameter of the performance index (PI) is
 423 better than F_v/F_M for measuring these effects. As shown in the studies conducted by Parolin
 424 (2001b), Waldhoff et al. (2002), Rengifo et al. (2005) and Maurenza et al. (2012), the values
 425 of F_v/F_M were only sensitive to flooding under extreme conditions. One possible explanation
 426 for this low sensitivity of F_v/F_M is that it only reflects a function of the observed maximum
 427 fluorescence of F_0 and F_M , whereas PI_{ABS} considers the maximum fluorescence intensity
 428 (Strauss et al. 2006).

429 The relationship between $\log(PI_{ABS})$ and $\log ET_o/ABS$ can be considered to be a
 430 characteristic property of the plant's ability to transform light energy into chemical energy
 431 (NADPH), which is directed into metabolic reactions in the biochemical processes of
 432 photosynthesis (Hermans et al. 2003). Linearity between the two log functions of the
 433 performance index (PI_{ABS}) and electron-transport activity (ET_o/ABS) makes it possible to
 434 determine the susceptibility and tolerance of different genotypes and species to different types
 435 of stress (Oukarroum et al. 2007). In the present study the same relationship was used to
 436 confirm the behavior of tolerant and intolerant species under flooded conditions (Fig. 5),
 437 demonstrating that intolerant species such as *Cc*, *Vg* and *Vj* had lower performance compared
 438 to tolerant species. This relationship also indicated that in *Gs* and *Ad* loss of leaves is one of
 439 the strategies used to tolerate flooding so that these species could be grouped into distinct
 440 categories. This strategy reflects a strong down-regulation to tolerate flooding by *Gs* and *Ad*.

441 In the present study, ten native tree species in two flood-tolerance groups were tested
 442 for differences in their physiological response and overall resistance to waterlogged
 443 conditions over two flooding periods. Flood-intolerant species were clearly affected by
 444 inundation, which caused a reduction in pigment content, a change in the shape of chlorophyll
 445 *a* fluorescence transients and a shift in JIP parameters such as yields and the performance
 446 index. These effects were also present in tolerant species that lose their leaves under flooding
 447 (*Alchornea discolor* and *Genipa spruceana*), but were more pronounced in flood-intolerant
 448 species (*Cecropia concolor*, *Vismia guianensis* and *Vismia japurensis*). Flood-tolerant
 449 species, including *G. spruceana* and *A. discolor*, had strategies that involved down-regulation
 450 of the electron-transfer reactions. In contrast, flood-intolerant species initially had a down-
 451 regulation of the photosynthetic processes induced by flooding, which depended on duration
 452 of inundation (generally a short time) and provoked a die-off of these species. According to
 453 these results, we suggest that the new parameters of the chlorophyll *a* fluorescence technique
 454 are of great value in detecting and screening the changes resulting from flooding in tolerant
 455 and intolerant species in natural and artificially flooded areas (dams). Thus, this technique can
 456 help to identify potentially flood-tolerant species to be introduced in reforestation projects in
 457 riparian areas and around reservoirs.

458

459 **Acknowledgements**

460

461 We thank Conselho Nacional de Desenvolvimento Científico e Tecnológico (CNPq);
 462 Fundação de Amparo à Pesquisa do Estado do Amazonas (FAPEAM), the Large-Scale
 463 Atmosphere-Biosphere Experiment in Amazonia (LBA), Instituto Chico Mendes (ICMBio),
 464 Manaus Energia, IBAMA and the entire team of the Plant Physiology and Biochemistry
 465 Laboratory at INPA. J.F.C Gonçalves and P.M. Fearnside acknowledge fellowships provided
 466 by CNPq.

467

468 **References**

469

- 470 Baker NR (2008) Chlorophyll fluorescence: A probe of photosynthesis in vivo. *Annu Rev*
 471 *Plant Biol* 59:89-113
- 472 Brazil MME (2011) Plano Decenal de Expansão de Energia 2020. MME (Ministério de Minas
 473 e Energia), Empresa de Pesquisa Energética. Brasília, DF, Brazil. 2 vols (In
 474 Portuguese)
- 475 Bussotti F, Desotgiu R, Cascio C, Pollastrini M, Gravano E, Gerosa G, Marzuoli R, Nali C,
 476 Lorenzini G, Salvatori E, Manes F, Schaub M, Strasser RJ (2011) Ozone stress in
 477 woody plants assessed with chlorophyll *a* fluorescence. A critical reassessment of
 478 existing data. *Environ Exp Bot* 73:19-30
- 479 Bussotti F, Strasser RJ, Schaub M (2007) Photosynthetic behavior of woody species under
 480 high ozone exposure probed with the JIP-test: A review. *Environ Pollut* 147:430-437
- 481 Duarte B, Santos D, Marques JC, Caçador I (2014) Biophysical probing of *Spartina maritima*
 482 photo-system II changes during prolonged tidal submersion periods. *Plant Physiol*
 483 *Biochem* 77:122-132
- 484 Ferreira CS, Piedade MTF, Franco AC, Gonçalves JFC, Junk WJ (2009) Adaptive strategies
 485 to tolerate prolonged flooding in seedlings of floodplain and upland populations of
 486 *Himatanthus sucuuba*, a central Amazon tree. *Aquatic Bot* 90:246-252
- 487 Ferreira CS, Piedade MTF, Junk WJ, Parolin P (2007) Floodplain and upland populations of
 488 Amazonian *Himatanthus sucuuba*: Effects of flooding on germination, seedling
 489 growth and mortality. *Environ Exp Bot* 60:477-483

- 490 Ferreira CS, Piedade MTF, Wittmann AO, Franco AC (2010) Plant reproduction in the central
491 Amazonian floodplains: challenges and adaptations. *AoB PLANTS*
492 doi:10.1093/aobpla/plq009
- 493 Force L, Critchley C, van Rensen J (2003) New fluorescence parameters for monitoring
494 photosynthesis in plants. *Photosyn Res* 78:17-33
- 495 Gardiner ES, Krauss KW (2001) Photosynthetic light response of flooded cherrybark oak
496 (*Quercus pagoda*) seedlings grown in two light regimes. *Tree Physiol* 21:1103–1111
- 497 Gonçalves JFC, Santos Junior UM, Nina Junior AR, Chevreuril LR (2007) Energetic flux and
498 performance index in copaiba (*Copaifera multijuga* Hayne) and mahogany (*Swietenia*
499 *macrophylla* King) seedlings grown under two irradiance environments. *Braz J Plant*
500 *Physiol* 19:171-184
- 501 Haldimann P, Strasser RJ (1999) Effects of anaerobiosis as probed by the polyphasic
502 chlorophyll a fluorescence rise kinetic in pea (*Pisum sativum* L.). *Photosyn Res* 62:7-
503 83
- 504 Hendry GAF, Price AH (1993) Stress indicators: chlorophylls and carotenoids. In: Hendry
505 GA, Grime JP (eds). *Methods in Comparative Plant Ecology*. Chapman & Hall,
506 London, pp 148-152
- 507 Hermans C, Smeyers M, Rodriguez RM, Eyletters M, Strasser RJ, Delhaye J-P (2003) Quality
508 assessment of urban trees: A comparative study of physiological characterisation,
509 airborne imaging and on site fluorescence monitoring by the OJIP-test. *J Plant Physiol*
510 160:81-90
- 511 Hidding B, Sarneel JM, Bakker ES (2014) Flooding tolerance and horizontal expansion of
512 wetland plants: Facilitation by floating mats? *Aquatic Bot* 113:83–89
- 513 Joliot P, Joliot A (2002) Cyclic electron transfer in plant leaf. *Proc Nat Acad Sci* 99:10209-
514 10214
- 515 Junk WJ (1989) Flood tolerance and tree distribution in central Amazonia. In: *Tropical Forest*
516 *Botanical Dynamics. Speciation and Diversity.*--Holm-Nielson, L.B., Nielsen, I.C.,
517 Balsev, H. (eds). London: Academic Press, pp 47-64
- 518 Junk WJ, Piedade MTF, Parolin P, Wittmann F, Schöngart J (2010) *Central Amazonian*
519 *Floodplain Forests: Ecophysiology, Biodiversity and Sustainable Management.*
520 *Ecological Studies*, Springer Verlag, Heidelberg.
- 521 Kalaji HM, Oukarroum A, Alexandrov V, Kouzmanova M, Brestic M, Zivcak M, Samborska
522 IA, Cetner MD, Allakhverdiev SI, Goltsev V (2014) Identification of nutrient
523 deficiency in maize and tomato plants by in vivo chlorophyll a fluorescence
524 measurements. *Plant Physiol Biochem* 81:16-25
- 525 Kissmann C, da Veiga EB, Eichemberg MT, Habermann G (2014) Morphological effects of
526 flooding on *Styrax pohlilii* and the dynamics of physiological responses during flooding
527 and post-flooding conditions. *Aquatic Bot* 119:7–14
- 528 Kozłowski TT (1997) Responses of woody plants to flooding and salinity. *Tree Physiol*
529 *Monog* 1:1–29
- 530 Kozłowski TT (2002) Physiological-ecological impacts of flooding on riparian forest
531 ecosystems. *Wetlands* 22:550-561
- 532 Lavinsky AO, Sant'Ana CD, Mielke MS, De Almeida A-AF, Gomes FP, França S, Silva DC
533 (2007) Effects of light availability and soil flooding on growth and photosynthetic
534 characteristics of *Genipa americana* L. seedlings. *New Forests* 34:41-50
- 535 Lázár D (2006) The polyphasic chlorophyll a fluorescence rise measured under high intensity
536 of exciting light. *Func Plant Biol* 33:9-30
- 537 Lichtenthaler HK, Wellburn AR (1983) Determination of total carotenoids and chlorophyll a
538 and b of leaf extracts in different solvents. *Biochem Soc Trans* 11:591-592

- 539 Maurenza D, Marenco RA, Parolin P, Piedade MT (2012) Physiological responses to flooding
540 and light in two tree species native to the Amazonian floodplains. *Aquatic Bot* 96:7–
541 13
- 542 Mielke MS, Schaffer B (2010) Leaf gas exchange, chlorophyll fluorescence and pigment
543 indexes of *Eugenia uniflora* L. in response to changes in light intensity and soil
544 flooding. *Tree Physiol* 30:45-55
- 545 Mielke MS, Schaffer B (2011) Effects of soil flooding and changes in light intensity on
546 photosynthesis of *Eugenia uniflora* L. seedlings. *Acta Physiol Plant* 33:1661–1668
- 547 Noodén LD, Guiamét JJ, John I (1997) Senescence mechanisms. *Physiologia Plantarum*
548 101:746-753.
- 549 Oliveira, V.C., Joly, C.A., 2010. Flooding tolerance of *Calophyllum brasiliense* Camb.
550 (Clusiaceae): morphological, physiological and growth responses. *Trees* 24:185–193
- 551 Oukarroum A, Madidi SE, Schansker G, Strasser RJ 2007 Probing the responses of barley
552 cultivars (*Hordeum vulgare* L.) by chlorophyll a fluorescence OLKJIP under drought
553 stress and re-watering. *Environ Exp Bot* 60:438-446
- 554 Parolin P (2001a) *Senna reticulata*, a pioneer tree from Amazonian várzea floodplains. *Bot*
555 *Review* 67(2):239-254
- 556 Parolin P (2001b) Morphological and physiological adjustments to waterlogging and drought
557 in seedlings of Amazonian floodplain trees. *Oecologia* 128:326-335
- 558 Parolin Pia, Waldhoff D, Zerm M (2010) Photochemical capacity after submersion in
559 darkness: How Amazonian floodplain trees cope with extreme flooding. *Aquatic Bot*
560 93:83–88
- 561 Pezeshki SR (1994) Plant response to flooding. In: Wilkinson RE (Ed.), *Plant/Environment*
562 *Interactions*. Marcel Dekker, New York, pp 289-321
- 563 Rengifo E, Tezara W, Herrera A (2005) Water relations, chlorophyll a fluorescence, and
564 contents of saccharides in tree species of a tropical forest in response to flood.
565 *Photosynthetica* 43:203-210
- 566 Santos Junior UM, Gonçalves JFC, Fearnside PM (2013) Measuring the impact of flooding on
567 Amazonian trees: photosynthetic response models for ten species flooded by
568 hydroelectric dams. *Trees*, 27: 193-210.
- 569 Sironval C, Strasser RJ, Brouers M (1981) Equivalence entre la theorie des flux et la theorie
570 des relations entre
571 proportions de pigments pour la description de la repartition de l'energie lumineuse absorbée
572 par les membranes photoactives. *Bull Acad R Belg* 67:248-259.
- 573 Smirnoff N (1993) The role of active oxygen in the response of plants to water deficit and
574 desiccation. *New Phytol* 125:27-58
- 575 Srivastava A (1997) Regulation of antenna structure and electron transport in Photosystem II
576 of *Pisum sativum* under elevated temperature probed by the fast polyphasic
577 chlorophyll a fluorescence transient: OKJIP. *Biochimica et Biophysica Acta-*
578 *bioenergetics* 1320:95-106
- 579 Stirbet A, Govindjee (2011) On the relation between the Kautsky effect (chlorophyll a
580 fluorescence induction) and photosystem II: basics and applications of the OJIP
581 fluorescence transient. *J Photochem Photobiol B Biol* 104(1-2):236-257
- 582 Strasser RJ, Govindjee (1992) On the O-J-I-P fluorescence transient in leaves and D1 mutants
583 of *Chlamydomonas reinhardtii*. In: Murata N (ed) *Research in Photosynthesis*. Kluwer
584 Academic Publishers, Dordrecht, The Netherlands, pp 29–32
- 585 Strasser BJ, Strasser RJ (1995) Measuring fast fluorescence transients to address
586 environmental questions: The JIP-test. In: Mathis P (ed), *Photosynthesis: from Light*
587 *to Biosphere*. Kluwer Academic Publishers, Dordrecht, pp 977–980

- 588 Strasser BJ (1997) Donor side capacity of Photosystem II probed by chlorophyll a
589 fluorescence transients. *Photosyn Res* 52:147-155
- 590 Strasser RJ, Srivastava A, Tsimilli-Michael M (1999) Screening the vitality and
591 photosynthetic activity of plants by fluorescence transient. In: Behl RK, Punia MS,
592 Lather BPS (eds), *Crop Improvement for Food Security*, pp.79-126. SSARM, Hisar.
- 593 Strasser RJ, Srivastava A, Tsimilli-Michael M (2001) The fluorescence transient as a tool to
594 characterize and screen photosynthetic samples. In: *Probing photosynthesis:
595 Mechanisms, regulation and adaptation*. --Yunus, M., Pathre, U., Mohanty, P., eds.
596 London: Taylor and Francis. pp. 445-483
- 597 Strasser RJ, Srivastava A, Tsimilli-Michael M (2004) Analysis of the chlorophyll a
598 fluorescence transient. In: *Photosynthesis and Respiration--Papageorgiou GC,
599 Govindjee* (eds). Dordrecht, The Netherlands: Springer, pp 321-362
- 600 Strauss AJ, Krüger GHJ, Strasser RJ, Heerden PDRV (2006) Ranking of dark chilling
601 tolerance in soybean genotypes probed by the chlorophyll a fluorescence transient O-
602 J-I-P. *Environ Exp Bot* 56:147-157
- 603 Tóth SZ, Schansker G, Strasser RJ (2005) In intact leaves, the maximum fluorescence level
604 (FM) is independent of the redox state of the plastoquinone pool: A DCMU-inhibition
605 study. *Biochim Biophys Acta (BBA) - Bioenergetics* 1708:275-282
- 606 Tsimilli-Michael M, Pêcheux M, Strasser RJ (1998) Vitality and stress adaptation of the
607 symbionts of coral reef and temperate foraminifers probed in hospite by the
608 fluorescence kinetics O-J-I-P. *Arch. Sci. Genève* 51:205-240.
- 609 Tsimilli-Michael M, Eggenberg P, Biro B, Köves-Pechy K, Vörös I, Strasser RJ (2000)
610 Synergistic and antagonistic effects of arbuscular mycorrhizal fungi and *Azospirillum*
611 and *Rhizobium* nitrogen-fixers on the photosynthetic activity of alfalfa, probed by the
612 polyphasic chlorophyll a fluorescence transient O-J-I-P. *Appl Soil Ecol* 15:169-182
- 613 Waldhoff, D., Furch, B., Junk, W.J., 2002. Fluorescence parameters, chlorophyll
614 concentration, and anatomical features as indicators for flood adaptation of an
615 abundant tree species in central Amazonia: *Symmeria paniculata*. *Environ Exper Bot*
616 48:225-235
- 617 Waldhoff D, Junk WJ, Furch B (1998) Responses of three Central Amazonian tree species to
618 drought and flooding under controlled conditions. *Internat J Ecol Environ Sci* 24:237-
619 252
- 620 Yamamoto, F., Kozłowski, T.T., 1987. Effects of flooding, tilting of stems, and ethrel
621 application on growth, stem anatomy and ethylene production of *Pinus densiflora*
622 Seedlings. *J Exper Bot* 38:293-310
- 623

624 **Table 1** Characteristics of the studied species.

Species and species abbreviation	Family	Successional status	Leaf phenology	625 626
<i>Cecropia concolor</i> ¹	<i>Cc</i> Cecropiaceae	Pioneer	Evergreen	627
<i>Vismia guianensis</i> ¹	<i>Vg</i> Hypericaceae	Pioneer	Evergreen	628
<i>Vismia japurensis</i> ¹	<i>Vj</i> Hypericaceae	Pioneer	Evergreen	629
<i>Alchornea discolor</i> ³	<i>Ad</i> Euphorbiaceae	Mid-successional	*	630 631
<i>Senna reticulata</i> ²	<i>Sr</i> Caesalpiniaceae	Mid-successional	Evergreen	632 633
<i>Brosimum lactescens</i>	<i>Bl</i> Moraceae	Late-successional	Evergreen	634 635
<i>Genipa spruceana</i> ³	<i>Gs</i> Rubiaceae	Late-successional	*	636 637
<i>Macrolobium angustifolium</i>	<i>Ma</i> Caesalpiniaceae	Late-successional	Evergreen	
<i>Nectandra amazonicum</i>	<i>Na</i> Lauraceae	Late-successional	Evergreen	
<i>Parinari excelsa</i>	<i>Pe</i> Chrysobalanaceae	Late-successional	Evergreen	

638 ¹*Cecropia concolor*, *Vismia guianensis* and *Vismia japurensis* are non-tolerant to flooding.639 ²*Senna reticulata* tolerated flooding inundation but doesn't tolerate submergence. See Parolin
640 (2001b)641 ³*Alchornea discolor* and *Genipa spruceana* can lose some of their leaves during flooding.

642 * When submitted to flooding these species can lose part of their leaves.

643

644
645**Table 2.** The JIP-test parameters, formulas and definitions

JIP test formulas	Definitions
<i>Extracted fluorescence parameters</i>	
$F_O = F_{50\mu s}$ (O)	Fluorescence intensity at 50 μs
$F_J = F_{2ms}$ (J)	Fluorescence intensity at 2 ms
$F_I = F_{30ms}$ (I)	Fluorescence intensity at 30 ms
$F_P = F_M$ (P)	Maximum fluorescence
$F_{100\mu s}$	Fluorescence intensity at 100 μs
$F_{300\mu s}$	Fluorescence intensity at 300 μs
T_{Fmax}	Time to reach F_M (ms)
<i>Calculated parameters</i>	
$F_v = (F_M - F_{50\mu s})$	Variable fluorescence
$V_K = (F_{300\mu s} - F_{50\mu s}) / (F_m - F_{50\mu s})$	Relative variable fluorescence at 300 μs
$V_J = (F_{2ms} - F_{50\mu s}) / (F_m - F_{50\mu s})$	Relative variable fluorescence at 2 ms
$V_I = (F_{30ms} - F_{50\mu s}) / (F_m - F_{50\mu s})$	Relative variable fluorescence at 30 ms
$OEC = 1 - (V_K / V_J)$	Oxygen evolving complex
$M_O = [4 \cdot (F_{300\mu s} - F_{50\mu s}) / (F_m - F_{50\mu s})]$	Net rate of PSII closure
Area	Area between the fluorescence curve and F_m
$S_M = (\text{area} / F_v)$	Normalized area
$S_M / T_{Fmax} \text{ ratio} = S_M / T_{Fmax}$	Average redox state, or Q_A^- / Q_A in the time span from 0 to T_{Fmax}
$N = S_M \cdot M_O \cdot (1 / V_J)$	Number of turnovers of Q_A
<i>Specific fluxes (Reaction Center: RC)</i>	
$ABS/RC = [(TR_O/RC) / (TR_O/ABS)]$	Effective antenna size of an active RC
$TR_O/RC = (M_O / V_J)$	Maximum trapping rate per RC
$DI_O/RC = [(ABS/RC) - (TR_O/RC)]$	Dissipation of an active RC
$ET_O/RC = [(TR_O/RC) (ET_O / TR_O)]$	Electron transport of an active RC
<i>Phenomenological fluxes (Cross section: CS)</i>	
ABS/CS Approximately proportional to F_O	Number of photons absorbed per CS
$TR_O/CS = (ABS/CS) (TR_O/ABS)$	Energy flux for trapping per CS
$DI_O/CS = (ABS/CS) - (TR_O/CS)$	Energy dissipation per CS
$ET_O/CS = (ET_O/RC) (RC/CS)$	Electron transport per CS
$RC/CS = (ABS/CS) (RC/ABS)$	Density of reaction centers per CS
<i>Yields</i>	
$\phi_{Po} (TR_O/ABS) = F_v / F_m = 1 - (F_{50\mu s} / F_M)$	Maximum quantum yield of primary photochemistry

$$\phi_{D_0} (DI_0/ABS) = DI_0/ABS = 1 - \phi_{P_0} = (F_{50\mu s} / F_M)$$

$$\Psi_0 (ET_0/TR_0) = 1 - V_J$$

$$\phi_{E_0} (ET_0/ABS) = \phi_{P_0} \cdot \Psi_0 = [1 - (F_{50\mu s} / F_M)] (1 - V_J)$$

Maximum quantum yield of non-photochemical de-excitation

Probability that a trapped exciton moves an electron further than Q_A^-

Probability that an absorbed photon moves an electron further than Q_A^-

Vitality index

$$PI_{ABS} = (RC/ABS) [\phi_{P_0} / (1 - \phi_{P_0})] [\Psi_0 / (1 - \Psi_0)]$$

Performance index

646 * For review see Strasser et al. (2004).

647

648

649 **Table 3** Effects of flooding on Chlorophyll *a* (Chl *a*); Chlorophyll *b* (Chl *b*); carotenoids (C_{x+c}); Chlorophyll total (Chl *a+b*); Chlorophyll *a* /
 650 Chlorophyll *b* ratio (Chl *a* / Chl *b*); Chlorophyll total / carotenoids ratio (Chl *a+b* / C_{x+c}) in ten tree tropical species in Central Amazonia. The
 651 species are: *Nectandra amazonicum* (*Na*); *Macrolobium angustifolium* (*Ma*); *Alchornea discolor* (*Ad*); *Brosimum lactescens* (*Bl*); *Senna*
 652 *reticulata* (*Sr*); *Genipa spruceana* (*Gs*); *Parinari excels* (*Pe*); *Cecropia concolor* (*Cc*); *Vismia guianensis* (*Vg*) and *Vismia japurensis* (*Vj*).

Species	Period	Chl <i>a</i> $\mu\text{mol m}^{-2}$	Chl <i>b</i>	Chl <i>a+b</i>	C _{x+c}	Chl <i>a</i> / Chl <i>b</i>	Chl <i>a+b</i> /C _{x+c}
<i>Na</i>	Non	617±81 A	242±50 A	860±128 A	208±25 A	2.59±0.30 B	4.14±0.38 A
	flooding						
<i>Ma</i>	Flooding	628±94 A	223±35 A	851±127 A	214±40 A	2.83±0.18 A*	3.99±0.30 A
	Non	421±84 A	135±38 A	557±120 A	162±29 A	3.18±0.33 A**	3.42±0.30 A
<i>Ad</i>	flooding						
	Flooding	437±101 A	156±41 A	594±141 A	169±36 A	2.82±0.21 B	3.50±0.22 A
<i>Bl</i>	Non	567±87 A	220±35 A	788±138 A	175±23 B	2.58±0.16 A	4.51±0.35 A***
	flooding						
<i>Sr</i>	Flooding	508±63 A	197±36 A	705±97 A	212±18 A***	2.61±0.24 A	3.32±0.35 B
	Non	535±89 A	208±50 A	742±138 A	182±20 A	2.62±0.26 A	4.07±0.45 A
<i>Gs</i>	flooding						
	Flooding	601±74 A	231±44 A	832±115 A	190±24 A	2.63±0.21 A	4.39±0.28 A
<i>Pe</i>	Non	432±93 A	166±53 A	597±145 A	138±29 B	2.71±0.27 A	4.31±0.34 A*
	flooding						
<i>Cc</i>	Flooding	482±51 A	149±35 A	676±83 A	175±24 A**	2.53±0.27 A	3.90±0.43 B
	Non	472±34 A**	186±28 A*	659±63 A**	156±8 A*	2.56±0.25 A	4.22±0.44 A
<i>Vj</i>	flooding						
	Flooding	344±117 B	138±48 B	482±164 B	122±36 B	2.50±0.15 A	3.99±0.82 A
<i>Vg</i>	Non	365±62 A	119±26 A	484±87 A	139±20 A	3.09±0.19 A*	3.49±0.40 B
	flooding						
<i>Vj</i>	Flooding	374±63 A	136±32 A	511±93 A	126±15 A	2.79±0.28 B	4.05±0.46 A**
	Non	468±107 A**	169±43 A	637±149 A*	195±39 A**	2.78±0.17 A**	3.25±0.37 A
<i>Vg</i>	flooding						
	Flooding	298±126 B	133±39 A	451±176 B	135±41 B	2.21±0.58 B	3.17±0.54 A

Vg	Non	434±86 A**	151±34 A*	585±114 A**	159±31 A**	2.92±0.55 A	3.69±0.36 A*
	<i>flooding</i>						
	Flooding	275±105 B	107±45 B	382±149 B	121±29 B	2.61±0.30 A	3.06±0.61 B
Vj	Non	542±108 A***	207±54 A	749±159 A**	195±35 A**	2.67±0.30	3.83±0.32 A
	<i>flooding</i>					A***	
	Flooding	375±76 B	177±36 A	553±107 B	161±19 B	2.14±0.36 B	3.44±0.61 A

653 Means of ten plants (\pm SD); mean values followed by the same letters between the flooding and non-flooding periods for the same species did not
654 differ at $P \leq 0.05$ by Student's *t*-test for data with parametric distributions, and Mann-Whitney *U*-test for data with non-parametric distributions.
655 Significant differences between the periods are indicated with a single asterisk ($P \leq 0.05$), double asterisk ($P \leq 0.01$) or triple asterisk, ($P \leq$
656 0.001).
657

658

659

660

661

662

663

664

Table 4. Effects of flooding on Maximum quantum yield of primary photochemistry (ϕ_{P_0}); Probability that a trapped exciton moves an electron further than Q_A^- (Ψ_0); Probability that an absorbed photon moves an electron further than Q_A^- (ϕ_{E_0}); Maximum quantum yield of non-photochemical de-excitation (ϕ_{D_0}); yield and density of reaction centers per cross section (RC/CS); and the performance index (PI_{ABS}) in ten tree tropical species in Central Amazonia. The species are: *Nectandra amazonicum* (*Na*); *Macrolobium angustifolium* (*Ma*); *Alchornea discolor* (*Ad*); *Brosimum lactescens* (*Bl*); *Senna reticulata* (*Sr*); *Genipa spruceana* (*Gs*); *Parinary excels* (*Pe*); *Cecropia concolor* (*Cc*); *Vismia guianensis* (*Vg*) and *Vismia japurensis* (*Vj*).

Species	Period	ϕ_{P_0}	Ψ_0	ϕ_{E_0}	ϕ_{D_0}	RC/CS	PI_{ABS}
<i>Na</i>	<i>Non flooding</i>	0.72±0.02 A	0.54±0.06 A	0.39±0.05 A	0.28±0.02 A	336±35 A	1.61±0.49 A
	<i>Flooding</i>	0.73±0.04 A	0.50±0.08 A	0.37±0.07 A	0.27±0.04 A	336±33 A	1.59±0.87 A
<i>Ma</i>	<i>Non flooding</i>	0.78±0.01 A	0.46±0.02 A	0.36±0.02 A	0.22±0.01 A	362±23 A	1.55±0.19 A
	<i>Flooding</i>	0.76±0.02 A	0.48±0.05 A	0.36±0.05 A	0.24±0.02 A	362±23 A	1.43±0.40 A
<i>Ad</i>	<i>Non flooding</i>	0.69±0.04 A**	0.44±0.06 A	0.31±0.06 A	0.31±0.04 B	268±13 A**	1.10±0.46 A*
	<i>Flooding</i>	0.63±0.03 B	0.41±0.05 A	0.27±0.04 A	0.37±0.03 A**	247±17 B	0.72±0.33 B
<i>Bl</i>	<i>Non flooding</i>	0.68 ±0.07 A	0.42±0.06 A	0.29±0.06 A	0.32±0.07 A	336±56 A	0.95±0.44 A
	<i>Flooding</i>	0.70±0.03 A	0.45±0.09 A	0.31±0.07 A	0.30±0.03 A	335±21 A	0.93±0.38 A
<i>Sr</i>	<i>Non flooding</i>	0.74±0.02 A	0.40±0.04 B	0.30±0.04 A	0.26±0.02 A	284±14 A	1.02±0.33 A
	<i>Flooding</i>	0.73±0.03 A	0.45±0.05 A*	0.33±0.04 A	0.27±0.03 A	291±32 A	1.12±0.37 A
<i>Gs</i>	<i>Non flooding</i>	0.74±0.02 A***	0.54±0.03 A**	0.40±0.03 A***	0.26±0.02 B	320±25 A***	1.50±0.30 A**
	<i>Flooding</i>	0.64±0.05 B	0.47±0.07 B	0.31±0.06 B	0.36±0.05 A***	225±23 B	0.93±0.36 B
<i>Pe</i>	<i>Non flooding</i>	0.73±0.02 A	0.43±0.05 A	0.32±0.04 A	0.27±0.02 A	395±26 A***	1.06±0.25 A
	<i>Flooding</i>	0.71±0.05 A	0.44±0.05 A	0.31±0.05 A	0.29±0.05 A	278±51 B	0.93±0.35 A
<i>Cc</i>	<i>Non flooding</i>	0.72±0.04 A**	0.51±0.08 A**	0.37±0.07 A**	0.28±0.04 B	299±48 A**	1.50±0.73 A**
	<i>Flooding</i>	0.61±0.10 B	0.33±0.16 B	0.22±0.12 B	0.39±0.10 A**	249±47 B	0.60±0.52 B
<i>Vg</i>	<i>Non flooding</i>	0.73±0.05 A**	0.52±0.08 A***	0.38±0.08 A***	0.27±0.05 B	299±24 A***	1.48±0.60 A***
	<i>Flooding</i>	0.58±0.13 B	0.30±0.15 B	0.20±0.11 B	0.42±0.13 A**	213±60 B	0.43±0.33 B
<i>Vj</i>	<i>Non flooding</i>	0.72±0.03 A***	0.51±0.07 A***	0.37±0.07 A***	0.28±0.03 B	320±30 A***	1.40±0.68 A***

<i>Flooding</i>	0.59±0.11 B	0.31±0.13 B	0.21±0.10 B	0.41±0.11 A***	245±43 B	0.48±0.35 B
------------------------	--------------------	--------------------	--------------------	--------------------------	-----------------	--------------------

665 Means of ten plants (\pm SD); mean values followed by the same letters between the flooding and non-periods for the same species did not differ at
666 $P \leq 0.05$ by Student's *t*-test for data with parametric distributions, and Mann-Whitney *U*-test for data with non-parametric distributions.

667 Significant differences between the periods are indicated with a single asterisk ($P \leq 0.05$), double asterisk ($P \leq 0.01$) or triple asterisk, ($P \leq$
668 0.001).

669

670

671

672

673 **FIGURE LEGENDS**

674 **Figure 1.** Mean values \pm standard deviation of reservoir water level (m) (a), precipitation (b)
 675 and minimum and maximum air temperature (c) in the region of Balbina Hydroelectric Dam
 676 (BHD) between 2005 and 2007. *information on non-flooding (blue) and flooding (red)
 677 periods are highlighted. Data obtained from Manaus Energia. The dashed lines refer to the
 678 flood and non-flood stage.

679
 680 **Figure 2.** Left: Average behavior of the fluorescence transients for each of the ten tree species
 681 is reported (mean of 50 leaves for each transient) both for the non-flooded period and during
 682 inundation. Right: The results of the JIP-test presented as “radar-plots” (each parameter is
 683 expressed as the mean of the ratio “flooded/non-flooded”. The value for the non-flooded
 684 period is used to standardize values under flooded conditions. Significant differences between
 685 the periods are indicated with a single asterisk ($P \leq 0.05$), double asterisk ($P \leq 0.01$) or triple
 686 asterisk ($P \leq 0.001$). Fluorescence intensity at 50 μs ($F_O = F_{50\mu\text{s}}$ (O)), 100 μs ($F_{100\mu\text{s}}$), 300 μs
 687 ($F_{300\mu\text{s}}$), 2 ms ($(F_J = F_{2\text{ms}}$ (J)) 30 ms ($F_I = F_{30\text{ms}}$ (I)) and maximum fluorescence (F_m (P));
 688 Number of turnovers of Q_A (N); The specific energy fluxes (activities per reaction center, RC)
 689 for absorption (ABS/RC), trapping (TRo/RC), electron transport (ETo/RC) and dissipation
 690 (DIo/RC) of an active RC; the corresponding activities per excited cross section (ABS/CS,
 691 TRo/CS, ETo/CS and DIo/CS); Area between the fluorescence curve and F_m (Area); Time to
 692 reach F_M (ms) ($T_{F_{\text{max}}}$); Normalized area ($S_M = (\text{area}/F_v)$) and Average redox state, or Q_A^-/Q_A in
 693 the time span from 0 to $T_{F_{\text{max}}}$ ($S_M/T_{F_{\text{max}}}$); Variable fluorescence (F_v); Relative variable
 694 fluorescence at 300 μs (V_K), 2 ms (V_J) and 30ms (V_I); Oxygen evolving complex (OEC); and
 695 Net rate of PSII closure (M_O). For details see Table 2.

696
 697 **Figure 3.** Left: For each species the average behavior of fluorescence transients normalized
 698 between O and P is reported (species means, $n = 50$ leaves), both for the flooded and non-
 699 flooded periods. Plots in the middle: for each species, change in the shape of the Chl *a*
 700 fluorescence transient curves is normalized between O and P (V_{OP}) - $\square V_{OP} = (V_{OP(\text{flooding})} -$
 701 $V_{OP(\text{non-flooding})})$. Plots on the right side: for each species, change in the shape of the Chl *a*
 702 fluorescence transient curve normalized between O and J (V_{OJ}) showing the K-band. $\square V_{OJ} =$
 703 $(V_{OJ(\text{sunlight})} - V_{OJ(\text{shade})})$.

704
 705 **Figure 4.** Specific relative changes (in %) in: (A) reaction centers per chlorophyll (RC/ABS);
 706 (B) efficiency of primary photochemistry [$\phi_{P_0}/(1 - \phi_{P_0})$]; and (C) efficiency of conversion of
 707 excitation energy to electron transport [$\Psi_0/(1 - \Psi_0)$] induced by flooding relative to the non-
 708 flooded period. These terms are variables in the performance index (see Appendix).
 709 Significant differences between the periods are indicated with a single asterisk ($P < 0.05$),
 710 double asterisk ($P < 0.01$) or triple asterisk ($P < 0.001$). The species are: *Nectandra*
 711 *amazonicum* (Na); *Macarlobium angustifolium* (Ma); *Alchornea discolor* (Ad); *Brosimum*
 712 *lactescens* (Bl); *Senna reticulata* (Sr); *Genipa spruceana* (Gs); *Parinary excels* (Pe);
 713 *Cecropia concolor* (Cc); *Vismia guianensis* (Vg) and *Vismia japurensis* (Vj).

714
 715
 716 **Figure 5.** Relationship between the log function of the relative performance index (Log
 717 $(PI_{\text{ABS}})_{\text{rel}}$ [=Log $(PI_{\text{ABS}}(\text{flooding}) / PI_{\text{ABS}}(\text{non-flooding}))$] and the relative yield of electron transport
 718 $(ET_{\text{O}}/ABS)_{\text{rel}}$ [= $(ET_{\text{O}}/ABS(\text{flooding}) / ET_{\text{O}}/ABS(\text{non-flooding}))$]. The species are: *Nectandra*
 719 *amazonicum* (Na); *Macarlobium angustifolium* (Ma); *Alchornea discolor* (Ad); *Brosimum*
 720 *lactescens* (Bl); *Senna reticulata* (Sr); *Genipa spruceana* (Gs); *Parinary excels* (Pe);
 721 *Cecropia concolor* (Cc); *Vismia guianensis* (Vg) and *Vismia japurensis* (Vj).

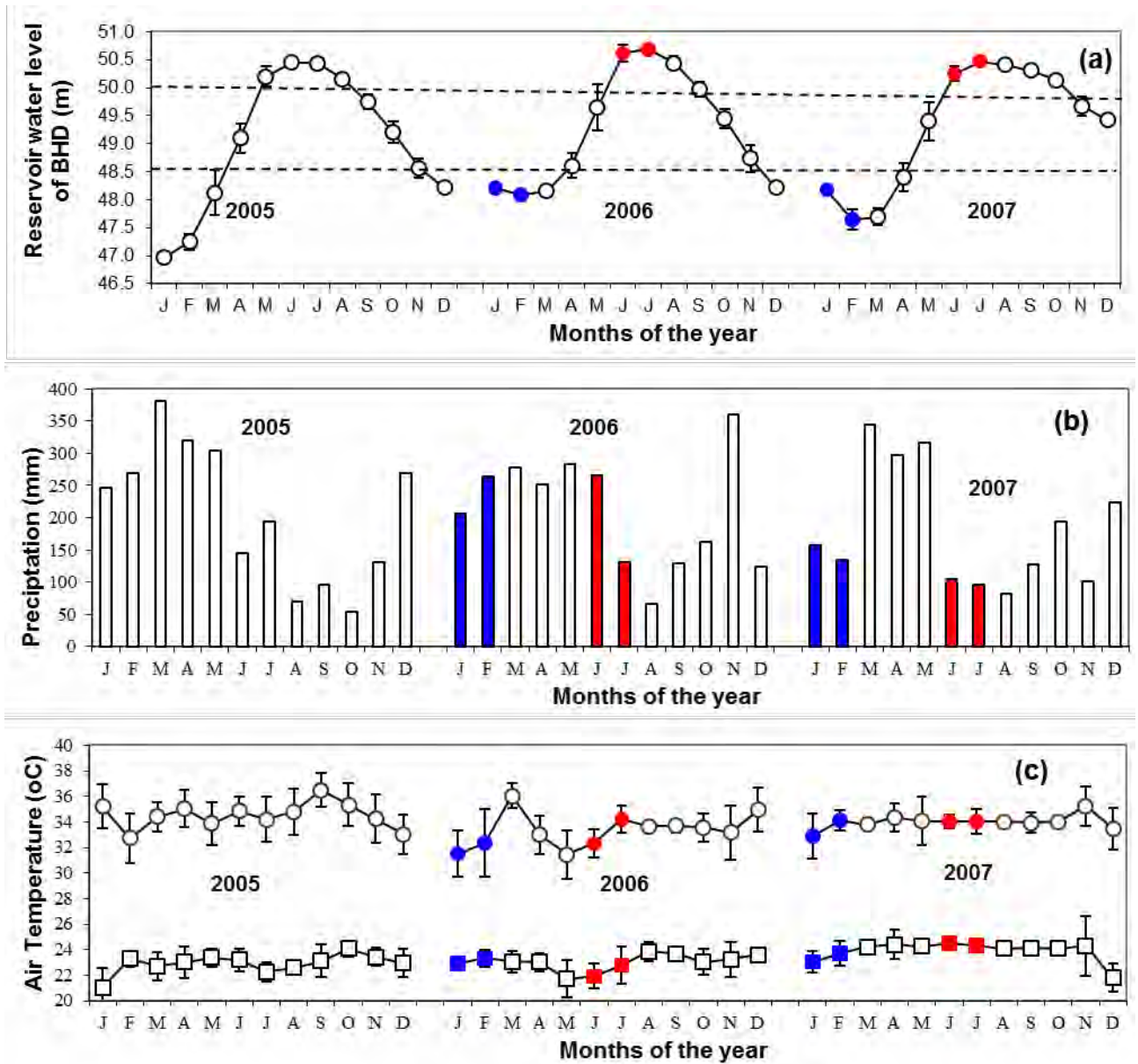


Figure 1

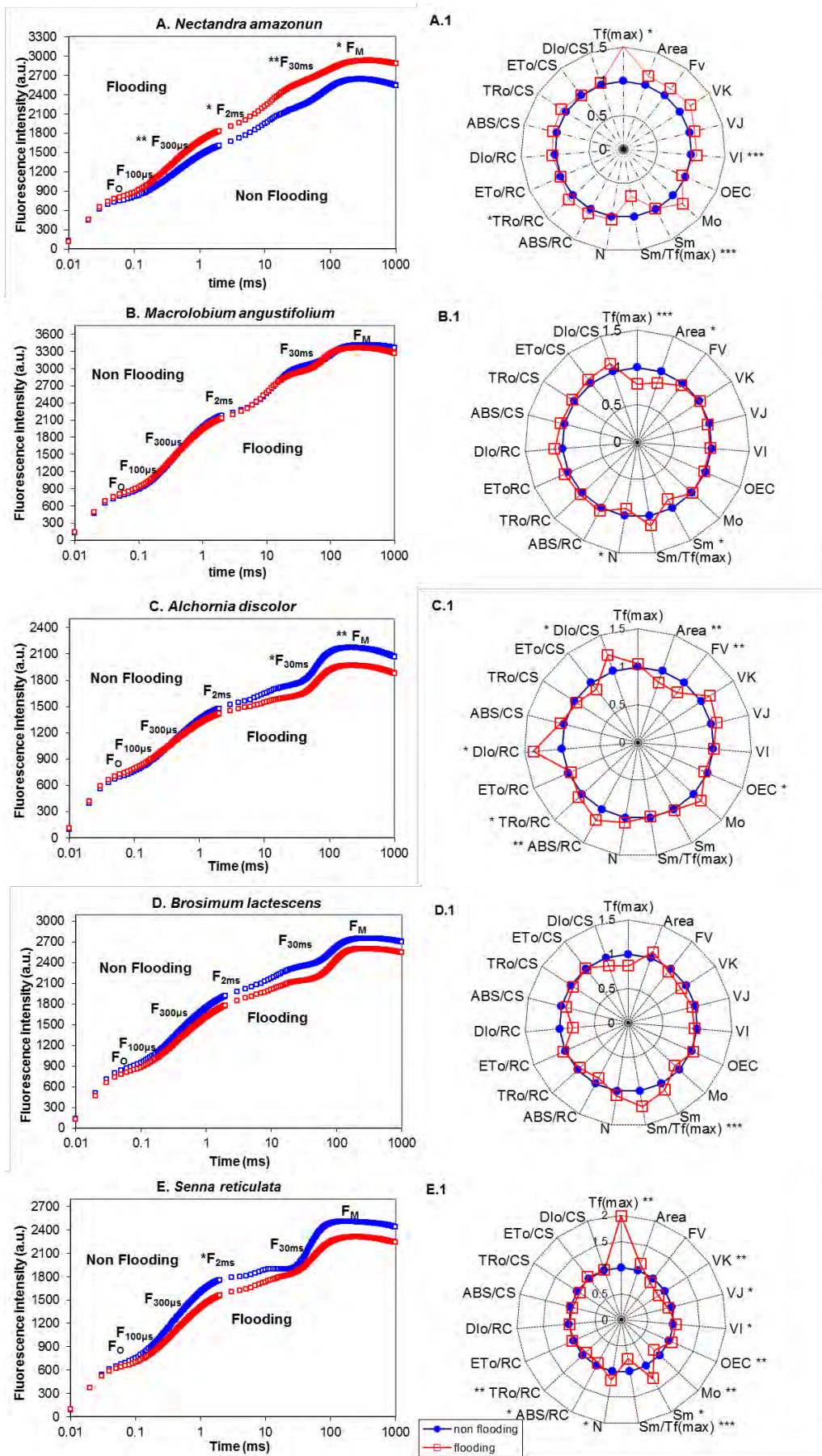


Figure 2

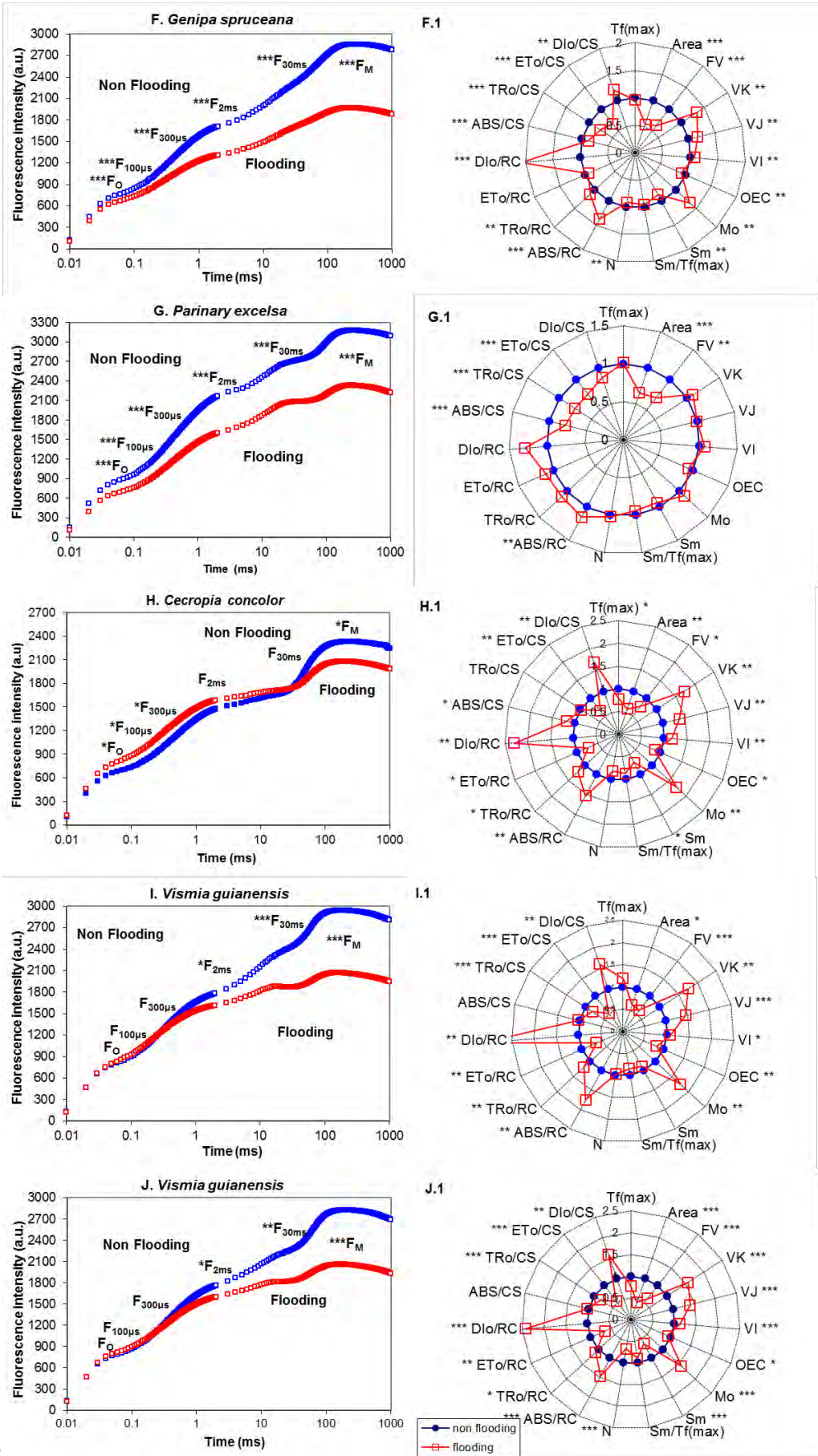


Figure 2

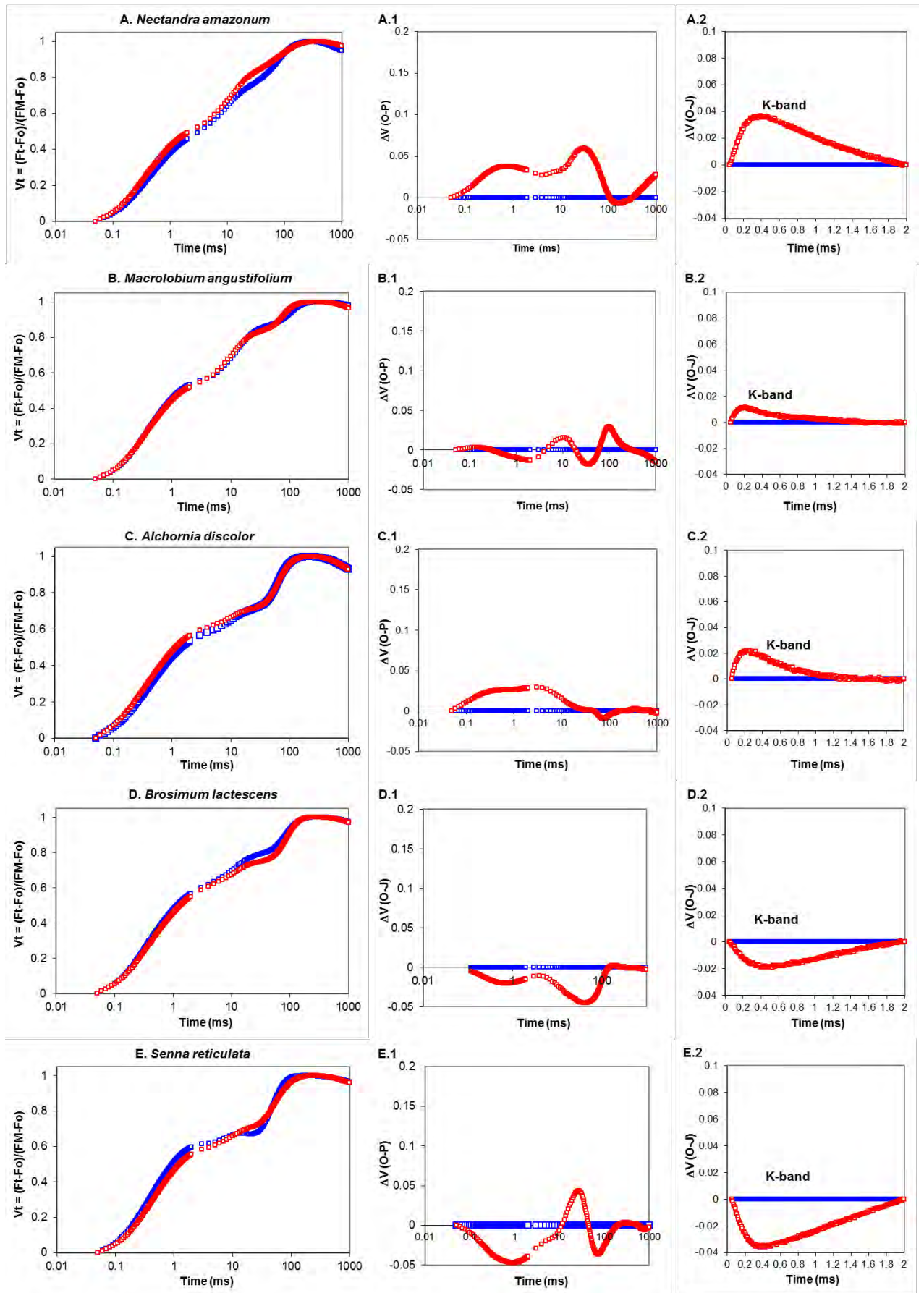


Figure 3

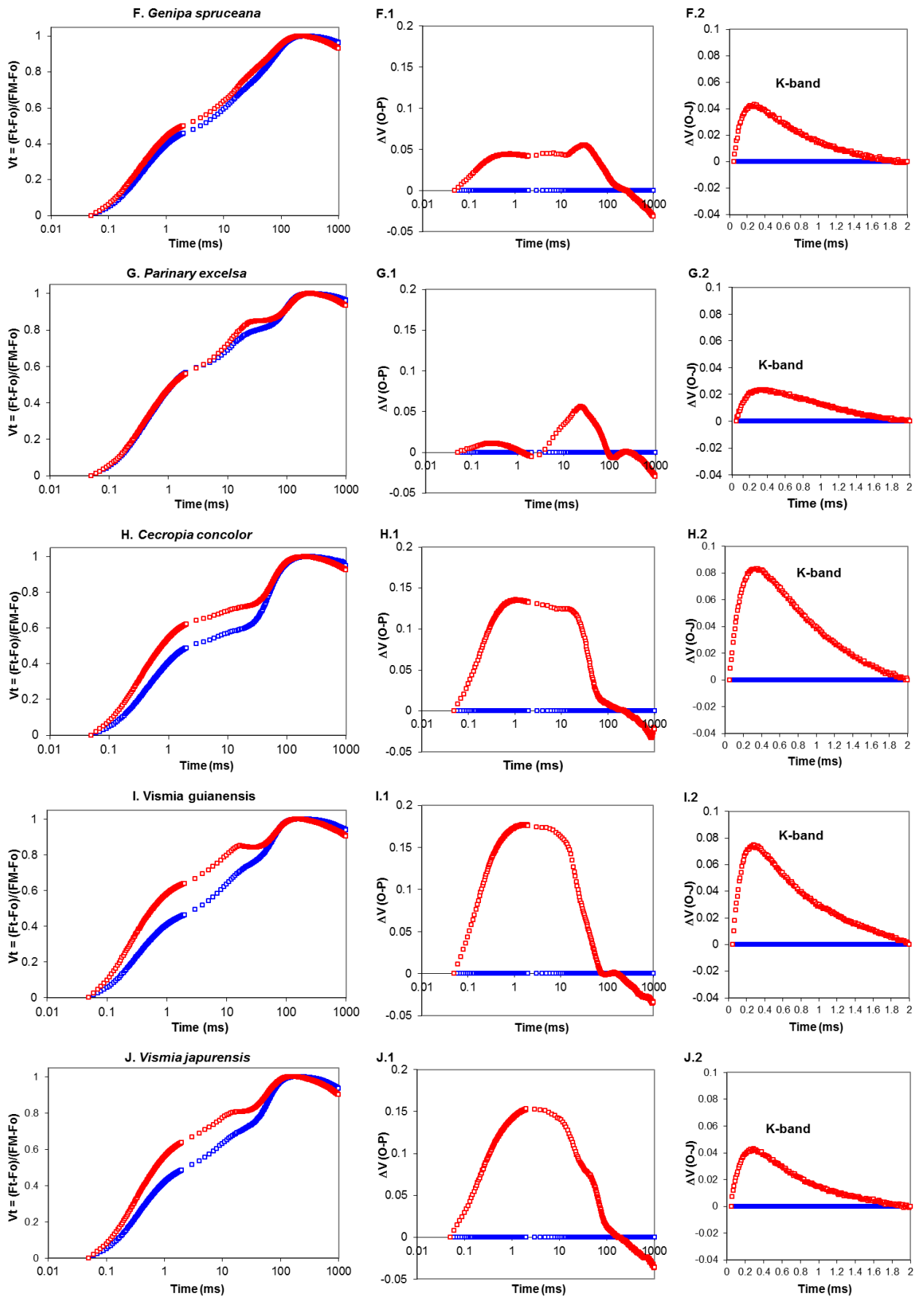


Figure 3

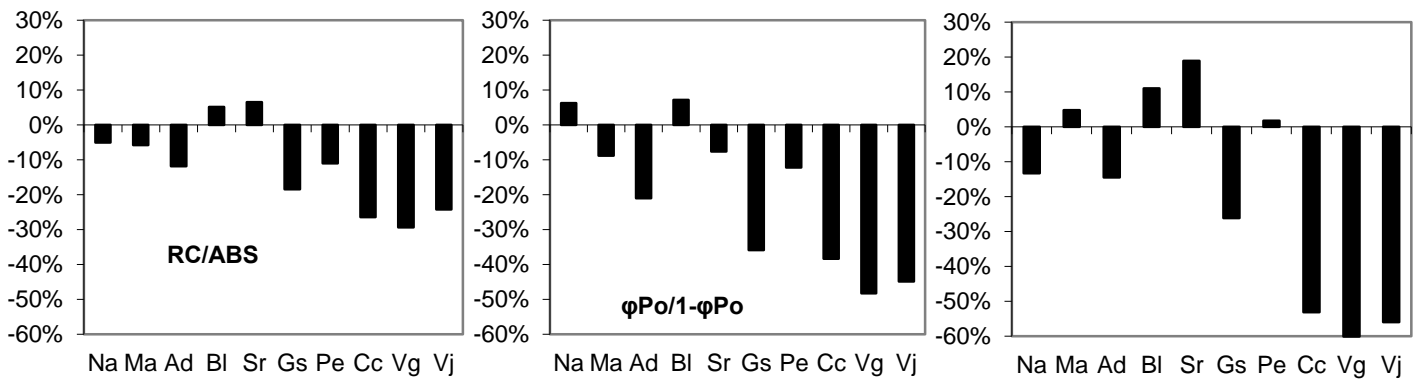


Figure 4

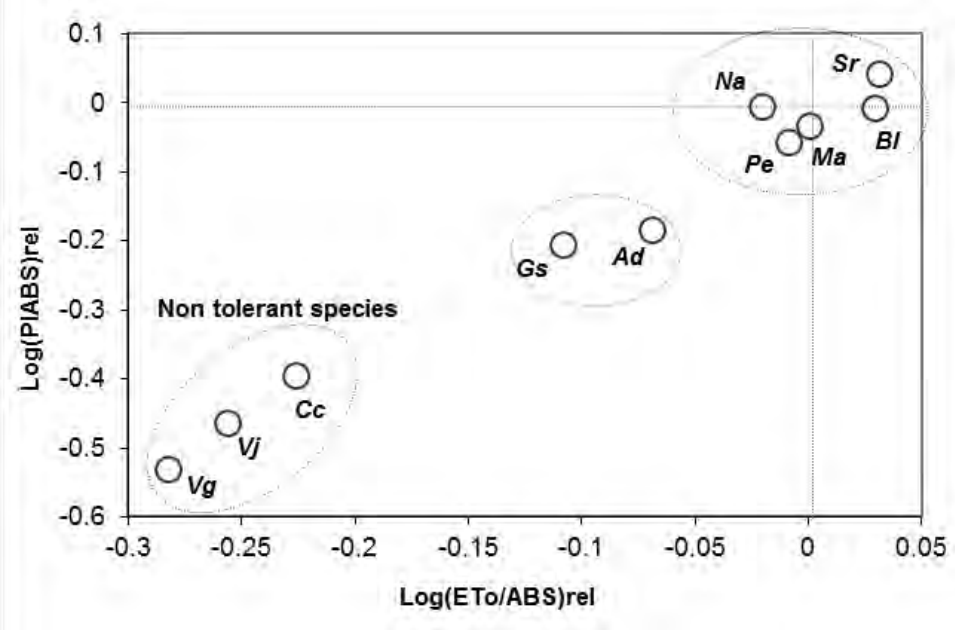


Figure 5